

Force Transfer by Implant Supported Bar Retained Overdentures Using Three Dimensional Photoelastic Stress Analysis

Sang Wan Shin, DDS, MPH, PhD, MSc.*/
Harold W. Preiskel, MSc, MDS, FDSRCS **/
Martin Sherriff, BSc, PhD, Grad PRI, ANCRT ***

Three photoelastic resin edentulous mandible analogues with two Brånemark titanium fixtures in the canine regions were constructed to evaluate the magnitude and direction of stresses resulting from two methods of employing bar attachments. After stress freezing under unilateral loading of 5Kg, three-dimensional photoelastic stress analysis was undertaken.

Bar attachments without spacers produced higher stresses on structures around the implant than designs with spacers. Torquing stresses induced by cantilevered extensions were surprisingly high and these torquing stresses were concentrated on the distocervical contact point and labio-apical contact point between the implant and the surrounding structures.

* Associate Professor, Department of Dentistry, Korea University Medical school, Seoul, Korea

** Consultant, Department of Prosthetic Dentistry, UMDS Guy's Hospital, London, UK

*** Lecturer, Department of Dental Material, UMDS Guy's Hospital, London, UK

Presented at the 5th Meeting of International College of Prosthodontists, Bürgenstock Switzerland, September 23-26, 1993 and the 9th Meeting of Academy of Osseointegration, Orlando USA, March 3-5, 1994.

The Abstract was published (*Int J Oral Maxillofac Implants* 1994;9:122-123).

The concept of an overdenture supported by osseointegrated implants has become accepted as an alternative treatment to that of a fixed prosthesis. There has been a recent trend toward the use of the implant as an overdenture abutment because the overdenture procedure has advantages that include aesthetics, economics, and versatility of application. Despite the availability of extensive long term results of fixed prostheses supported by osseointegrated implants, similar information on overdentures incorporating attachments is relatively scarce.

Osseointegrated implants are not lined by a connective tissue sheath and are analogous to an ankylosed tooth.¹ Loads are transferred directly from the prosthesis to the bone as there is no periodontal ligament to act a damping or stress distributing mechanism. Correct design of the superstructure is thus critical. The design of bar attachments with distal cantilevered extensions has become popular, but Engquist² has suggested that the cantilever effect of bar attachments can cause higher bending moments, depending on the retention system. He suggested that if the female part permitted a small rotational movement, the bending moment from vertical load could be ignored.

It has been hypothesized that the stress generated by the attachment retaining the overdenture tends to be shared by the abutment fixtures and the edentulous ridge depending upon the retentive and supportive capability of the attachments, and that the rigid type of bar attachment (without spacer) might produce higher stress concentration compared with the resilient type (with spacer). It appeared that it would be valuable to analyse the effect of the spacer of the bar attachment with distal cantilevered extensions upon the stress characteristics on the surrounding structures of the osseointegrated implant.

The aims of this study were to evaluate the location and intensity of the stresses on the surrounding structures of osseointegrated implants supporting bar retained overdentures, to ascertain the effect of the spacer within bar attachments with cantilevered extensions upon

these structures, and to evaluate the suitability of cantilevered extensions of bar attachment as a superstructure for osseointegrated implants supporting overdentures.

MATERIAL AND METHODS

Three-dimensional stress analysis was undertaken to evaluate the magnitude and direction of stresses induced in photoelastic resin analogue mandibles using different clip to bar connections in bar attachments with cantilever extensions. This technique was chosen because it provided a visual display of stress to the surrounding structure of the osseointegrated implants supporting overdentures.

A model representing a patients edentulous mandible was made of embedding resin (Alec Tiranti Ltd. Reading, Berks RG7 5AR UK). The dimensions of this model were based on a dry skull. Two connected Bränemark implants (Nobelpharma, SDCA 018 S-402 26 Göteborg Sweden) 13mm x 3.75mm and transmucosal abutments (Nobelpharma, SDCA 005 S-402 26 Göteborg Sweden) 5.5mm long were placed in the canine regions of the master model. Three photoelastic epoxy resin models with implants and transmucosal abutments were duplicated by Epicote 828(Shell chemical Co. Cheter, CH4 9QA UK) with a Jeffamine hardner(Texaco Ltd. Lodon SWIX 7QJ UK). The alveolar ridge areas of the photoelastic resin mandible were covered with layers of silicone rubber, 2 mm thickness in the anterior and premolar regions, 3 mm in the molar regions, and 4 mm in the retromolar areas to simulate the masticatory mucosa. The experi-

mental dentures were made with self cure acrylic resin (Davis Schotlander & Davis Ltd. UK) by a copy denture technique with laboratory silicone putty (Coltene, Switzerland).

A Dolder bar was employed to connect the two implants and CM bars 5 mm in length as a distal cantilever each side. The long axis of each cantilevered bar was parallel with the longitudinal axis of the posterior residual ridge. The bars were connected to the gold cylinders (Nobelpharma, DCA 072 S-402 26 Göteborg Sweden) with sticky wax and were invested in soldering investment material (Speed E No. 04701, Whip Mix Co. Hartford, Connecticut USA). After drying the solder block, the soldering was carried out with flux (Ney Co. USA) and solder (Neocast 2, Cendres & Metaux, Bienne CH-2501 Switzerland) in the reducing zone of the blow torch. The assembly of the gold cylinders and the bars was fitted and connected with the gold screws (Nobelpharma, DCA 075 S-402 26 Göteborg Sweden) on the transmucosal abutments (Fig.1).

In order to create a space between the occlusal surface of the gold cylinders and the denture base, both gold cylinders were covered with wax 2mm thick. This space prevented binding of these components during loading. The spaces between the bar and ridge were filled with wax to prevent any material flowing under the bars, thereby making removal of the denture difficult. An access window was made in the denture on the corresponding lingual side before it was seated on the photoelastic resin mandible with the bar attachments. The sleeves were fixed to the denture with inlay pattern resin (Duralay

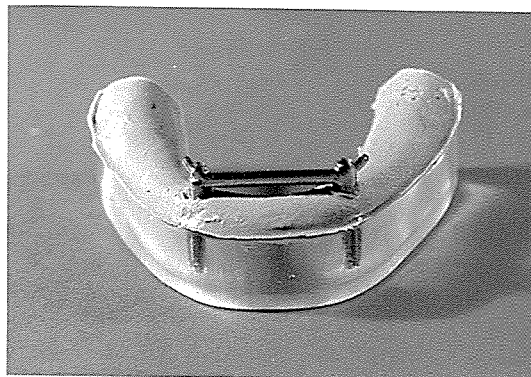


Fig. 1 The experimental photoelastic resin model and bar attachments

Main bar : Dolder bar, height 3.0mm ;
Spacer, thickness 1.05mm. Cantilevered
bar : CM bar, diameter 1.9mm ; Spacer,
thickness 0.5mm

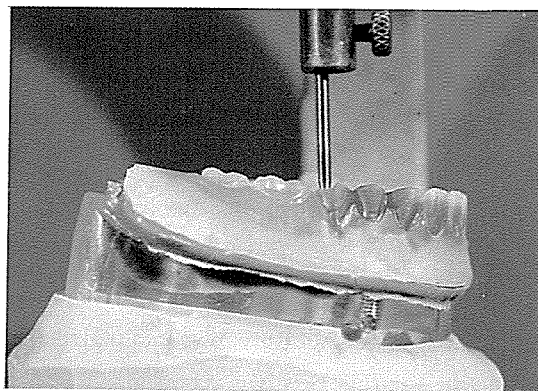


Fig. 2 The design of the bar joint

Model 1 : rigid design, Model 2 : moderate design, Model 3 : resilient design

Reliance Dental MFG. Worth, ILL 60482 USA). Figure 2 shows the distribution of spacers when they were employed.

It was necessary to construct a cushioned mounting table that would accept the photoelastic models and keep them in a constant relationship with the linear loading device (Fig. 3). This was accomplished by laboratory silicone putty. This provided a support for all the test models used throughout this study without

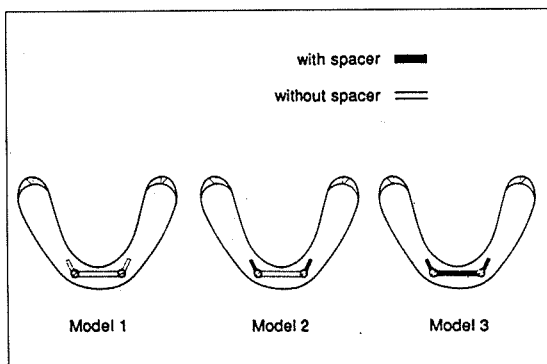


Fig. 3 Silicone rubber mounting table and shaft of the linear loading device.

producing any stress in the base and also gave a reproducible loading position.

The photoelastic model was stress-relieved or postured at 65°C and cooled slowly to room temperature for 8 hours. The postured model on the mounting table was placed on the base of the linear loading device with the metal loading shaft. The entire assembly was placed into the electronic oven and preheated to a temperature of 56°C at the rate of 1°C per minute. This temperature was maintained for one hour. At this time the metal loading shaft was activated on the flat surface of the right premolar with a load of 5 Kilograms. The temperature was maintained for another one hour under the load. The oven was then turned off and allowed to return to room temperature at a slow rate for 7 hours.

The labial and buccal views of the model under polarized light were observed with a Polariscope (Photoelastic Inc. PA, USA) and fibreoptic light (KL 1500-T, Schott, Germany). Sections, 8 mm in thickness of six regions were made for analysis in each model. Sections were undertaken labio-lingually from the surround-

ing structure of the implant fixture, bucco-lingually from the mandible under the second premolar and the second molar of the loaded and non-loaded sides. Each section was polished with abrasive papers (No.1000) under water in order to render it smooth and transparent. The sections were then observed with the polariscope. The margin of fringes on the surrounding structure of the implant of the loaded side were drawn with computer graphics.

RESULTS

Data were collected and reported as the number of fringes or fractions of fringes in the MESIO-DISTAL direction and the LABIO-LINGUAL direction.

1. Labial and buccal observation of the models in the MESIO-DISTAL direction

The fringe values measured were slightly different depending upon design on the cervical region in the loaded side while they were not different on the apical region in the loaded side and in the non-loaded side (Fig. 4a, b).

The observation points were numbered alphabetically on the contact area between the implant and the surrounding structure as follows (Fig. 5);

- A- Distal point in the cervical region of loaded side.
- B- Distal point in the apical region of loaded side.
- C- Centre point in the apical region of loaded side.
- D- Mesial point in the apical region of loaded side.
- E- Mesial point in the cervical region of loaded side.
- F- Mesial point in the cervical region of non-loaded side.

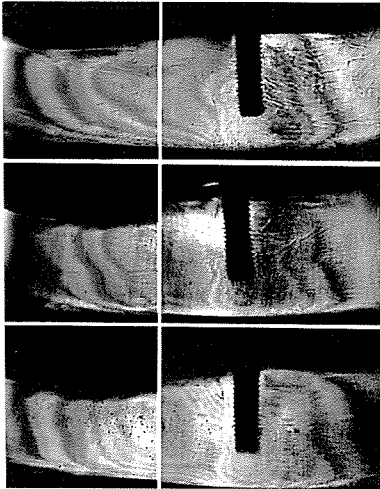


Fig. 4a Loaded side of the photoelastic resin models: top, model 1; middle, model 2; bottom, model 3.

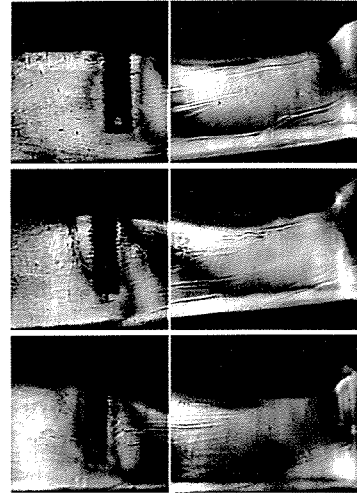


Fig. 4b Non-loaded side of the photoelastic resin models: top, model 1; middle, model 2; bottom, model 3.

- G- Mesial point in the apical region of non-loaded side.
- H- Centre point in the apical region of non-loaded side.
- I- Distal point in the apical region of non-loaded side.
- J- Distal point in the cervical region of non-loaded side.

Results observed under the circular set up of polariscope were reported in Table 1 and Fig. 6.

LOADED SIDE

The fringe orders and patterns of the stress concentration throughout the body of the mandibles were similar in the three models (Fig. 4a).

Surrounding structures of the implants

Total stresses measured on the surrounding structures of the implants of the loaded sides were similar in the three models. In the comparison of the fringe values between the mesial sides and the distal sides of the interface areas, the values were the same in the apical

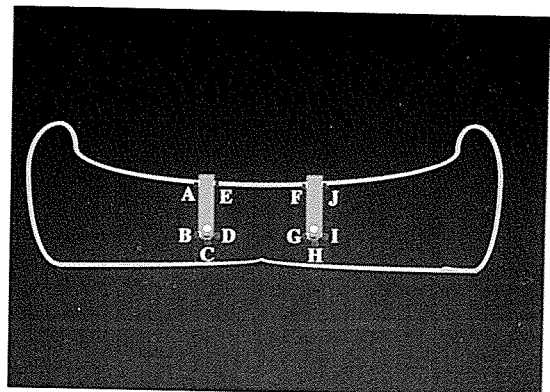


Fig. 5 Observation points between the implant and the surrounding structure in the mesio-distal direction

regions. However, the fringe values of the disto-cervical contact points were higher than those of the mesio-cervical contact points. The fringe-values on the disto-cervical contacts were similar in each model.

Residual ridge

The greatest stress on the residual ridge was

generated by model 3 (resilient design, with spacers on the Dolder bar and cantilevered extensions) and the smallest stress was generated by model 1 (rigid design, without spacers).

NON-LOADED SIDE

The models showed little difference of fringe values between the area of stress concentration

Table 1. Fringe values and their percentages on the Resin/Implant contact points Mesio-Distally.

	<u>Model 1</u>		<u>Model 2</u>		<u>Model 3</u>	
<u>Loaded side</u>	Value	Percentage	Value	Percentage	Value	Percentage
A	2.0	8.5	2.0	8.7	1.5	6.3
B	5.0	21.3	5.0	21.7	5.0	20.8
C	6.5	27.7	6.0	26.1	6.5	27.1
D	5.0	21.3	4.5	19.6	5.0	20.8
E	1.0	4.3	1.0	4.3	1.0	4.2
<u>Non-loaded side</u>						
F	1.0	4.3	0.5	2.2	1.0	4.2
G	0.5	2.1	1.0	4.3	0.5	2.1
H	0.5	2.1	1.0	4.3	1.0	4.2
I	1.0	4.3	1.5	6.5	1.5	6.3
J	1.0	4.3	0.5	2.2	1.0	4.2
Total	23.5	100.0	23.0	100.0	24.0	100.0

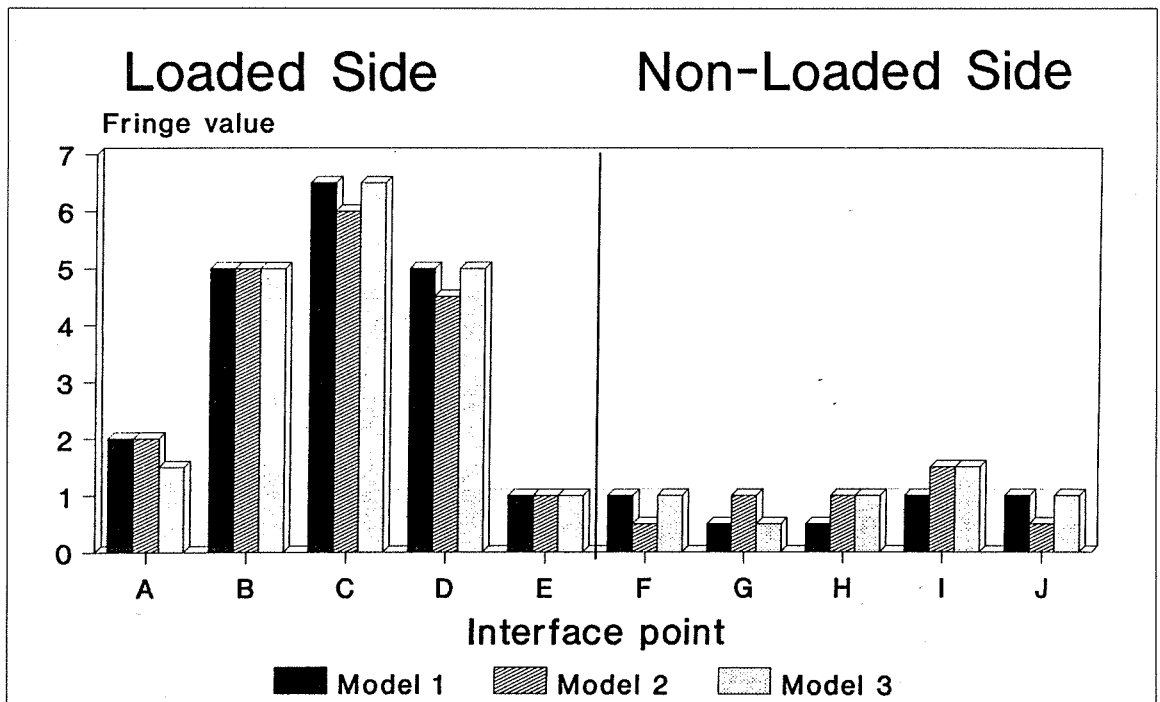


Fig. 6 Comparison of fringe values on the Resin/Implant contact points Mesio-Distally.

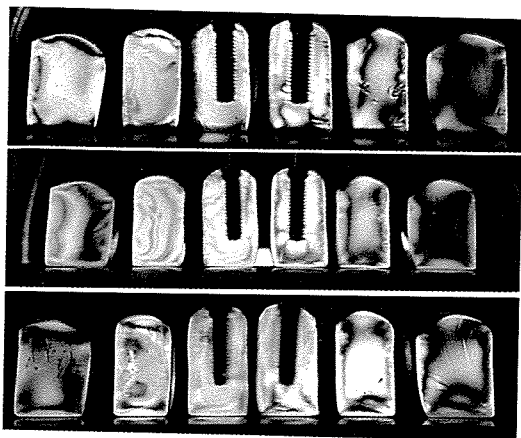


Fig. 7 Sections through the photoelastic resin mandible: top, model 1; middle: model 2; bottom, model 3.

in the surrounding structures of the implant fixtures and the residual ridges (Fig. 4b).

2. Observation of the sectioned models in the LABIO-LINGUAL direction

The fringe values measured were different depending upon design in the loaded side while they were not different in the nonloaded side (Fig. 7, 8).

The observation points were numbered alphabetically on the contact area between the implant and the surrounding structure as follows(Fig. 10);

- a- Labial point in the cervical region of loaded side.
- b- Labial point in the apical region of loaded side.
- c- Centre point in the apical region of loaded side.
- d- Lingual point in the apical region of loaded side.
- e- Lingual point in the cervical region of loaded side.
- f- Lingual point in the cervical region of non-loaded side.
- g- Lingual point in the apical region of non-loaded side.
- h- Centre point in the apical region of non-loaded side.

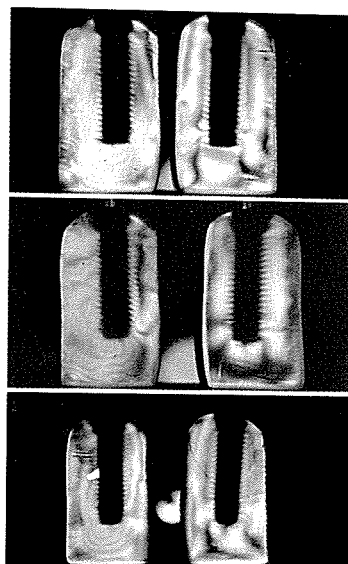


Fig. 8 Sections on the surrounding structure of the implant: top, model 1; middle, model 2; bottom, model 3.

- i- Labial point in the apical region of non-loaded side.
- j- Labial point in the cervical region of non-loaded side.

The fringe value and ones percentage for each point in the labio-lingual sections of the loaded and non-loaded sides were reported in Table 2 and Fig. 11.

LOADED SIDE

There were differences between the models of the fringe orders and patterns of the stress concentration on the labio-lingual sections.

Surrounding structure of the implant

While the fringe values on the Resin/ Implant contact points of the loaded side were almost the same between the mesio-distal and the labio-lingual planes, the fringes were closer labio-lingually than mesio-distally(Fig. 4a, 9).

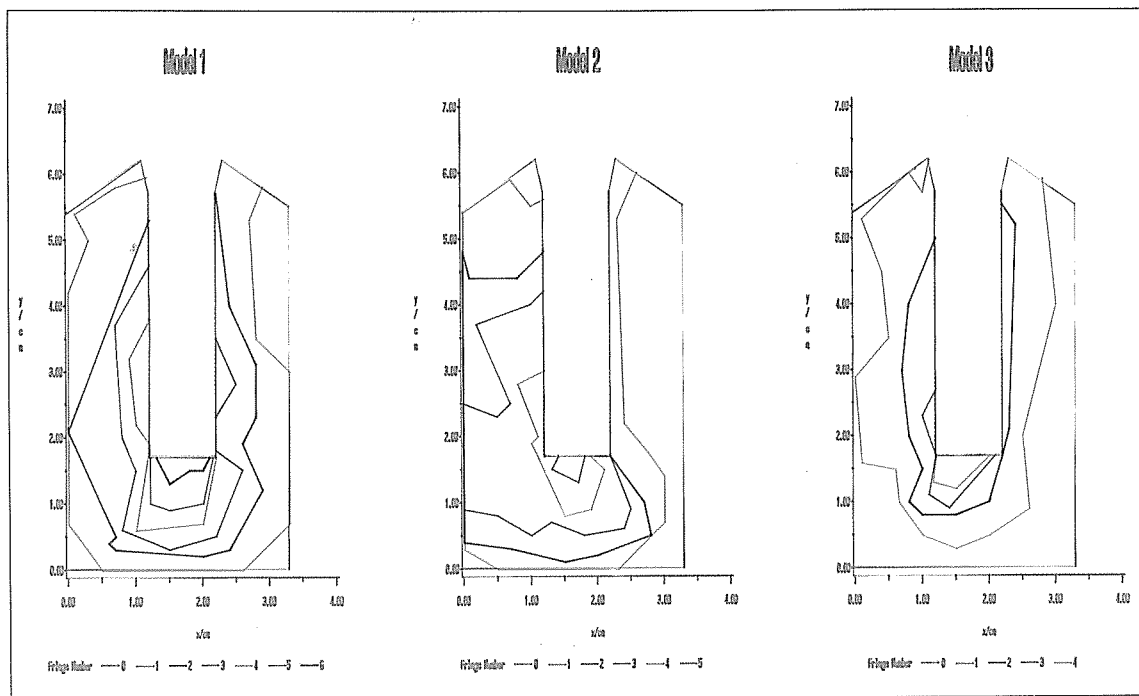


Fig. 9 Computer graphics with fringe numbers on the surrounding structures of the implant on the loaded side. Labio-lingual section, lingual on the right.

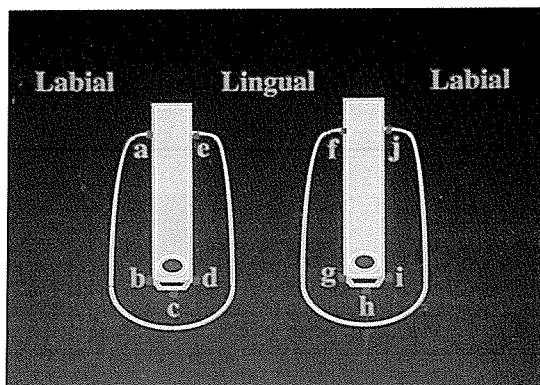


Fig.10 Observation points between the implant and the surrounding structure in the labio-lingual direction

Total fringe values measured on the surrounding structure of the implant differed according to the design of the bar joint (Table 2). The greatest fringe value was obtained in model 1 (rigid design, without spacers) and smallest

value in model 3 (resilient design, with spacers on the Dolder bar and cantilevered extensions).

A comparison of the fringe values between the labial side and lingual side of the interface area, showed a difference in the cervical and apical regions. However the fringe values of the labio-apical contact points were significantly higher than those of the linguo-apical contact points (Fig 8, 9). The torquing stresses were generated by all the models and the greatest fringe value was produced in the labio-apical contact point of the model 1 (rigid design) and the smallest in the model 3 (resilient design).

Residual ridge

The fringes of stress concentration were extended to the second molar region in the model 1 and 2, and to the second premolar

Table 2. Fringe values and their percentages on the Resin/Implant contact points Labio-Lingually

<u>Loaded side</u>	<u>Model 1</u>		<u>Model 2</u>		<u>Model 3</u>	
	Value	Percentage	Value	Percentage	Value	Percentage
A	1.5	6.8	1.0	5.7	1.0	6.2
B	4.5	20.5	4.0	22.9	3.0	18.8
C	6.5	29.5	5.5	31.4	4.5	28.1
D	3.5	25.9	2.0	11.4	1.5	9.4
E	2.0	9.1	1.0	5.7	1.5	9.4
<u>Non-loaded side</u>						
F	1.0	4.5	1.0	5.7	1.0	6.2
G	0.5	2.3	0.5	2.9	1.0	6.2
H	0.5	2.3	0.5	2.9	0.5	3.1
I	1.0	4.5	1.0	5.7	1.0	6.2
J	1.0	4.5	1.0	5.7	1.0	6.2
Total	22.0	100.0	17.5	100.0	16.0	100.0

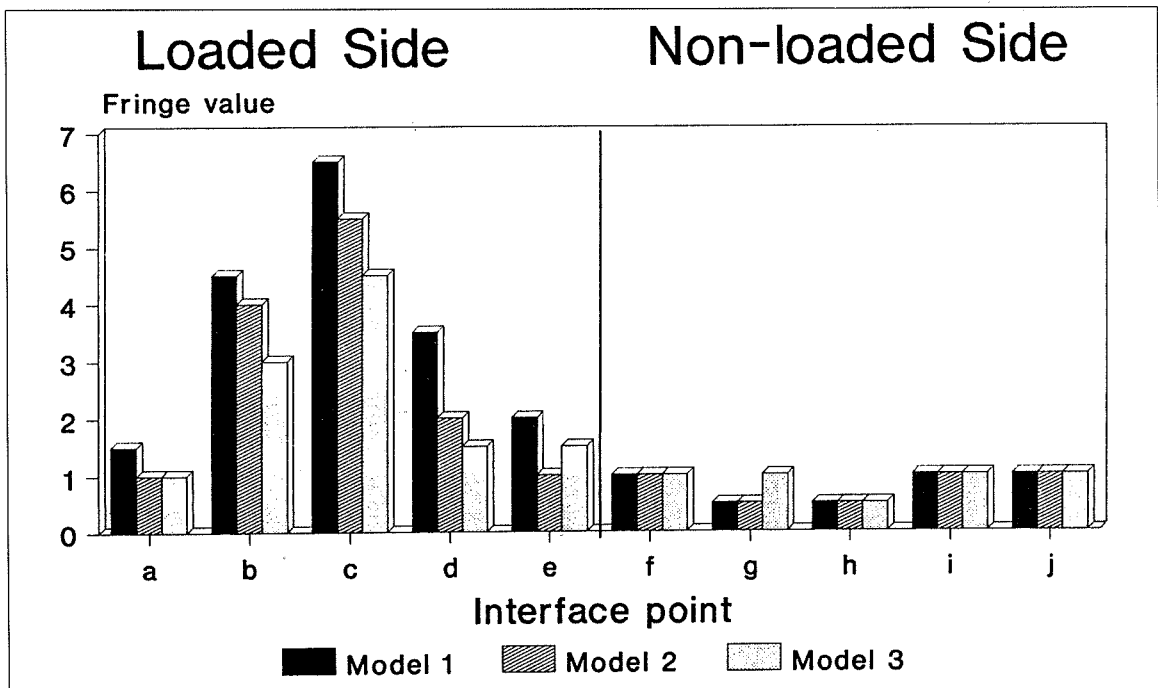


Fig. 11 Comparison of fringe values on the Resin/Implant contact points Labio-Lingually.

region in the model 3.

NON-LOADED SIDE

The models showed little difference of the

fringe orders and the patterns of stresses in the surrounding bone of the implant fixtures and the residual ridges (Fig. 7).

DISCUSSION

Due to the complex geometry of dental and oral structures, most stress analysis in dentistry has been studied *in vitro*. Caputo and Standlee³ stated that the three-dimensional and the quasi-three-dimensional photoelastic stress analysis were very useful techniques to elucidate stresses on the supporting tissues of restorations or prostheses. However, they pointed out that since the experimental approaches were virtually impossible to model all aspect of material behavior, the results could not be same as those in the living structures. Our study suffers similar constraints as several assumptions must be made in the evaluation of the results obtained using these types of models.

Photoelastic stress analysis may be reliable for homogeneous solids or composites. The photoelastic substance, Epicote 828, which was used to simulate bone is a homogeneous substance while bone is not. Physical properties of the simulated mucosa are different from those of the oral mucosa while the direction of the applied forces may also differ. Three-dimensional stress analysis of the supporting structures associated with a dental prostheses may have other limitations. Several construction and conversions are required to produce the experimental samples and conditions. In spite of these inherent problems, the fringe pattern obtained in pilot study supports the contention that the stresses incurred within an experimental model were reasonably consistent in terms of position and magnitude.

Of the total fringe values measured in the

surrounding structure of the implants, about eighty per cent of the load was distributed to the loaded side and about twenty per cent to the non-loaded side. The distribution of the occlusal load across the arch was similar in all the models. It appeared that the denture rotated laterally under unilateral loading. The values of the fringe orders on the surrounding bone of the implants of the loaded sides were lower in the cervical regions than those in the apical regions in both the mesiodistal plane and labio-lingual planes. It appeared that the vertical load on the second premolar region did not produce any excessive torquing. Our results agreed with those of Kinni et al⁴ who showed that with the Bränemark fixture there was no excessive stress concentration in the cervical region under vertical load.

While total fringe values on the Resin/Implant contact points of the loaded side were almost same in the plane of observation, the fringes on the surrounding structure of the implant were considerably closer labio-lingually than mesio-distally. They may indicate that the shear stresses on the Resin/Implant contact points of the loaded side were similar in both planes, but the degree of stress concentration around the implant of the loaded side was higher labio-lingually than mesio-distally.

Total fringe values measured around the implant depended upon design of the bar joint labio-lingually but not mesio-distally. The greatest value was observed in the rigid design and the lowest value in the resilient design labio-lingually. This may indicate that stresses observed in the model 3 (resilient design with spacers) were more evenly distri-

buted around the implant and residual ridge of the loaded side. It appeared that the thickness of the spacers of the bar attachments effected these results, and the spacers of the cantilever extensions (CM bar) effected the stress concentration mesio-distally and the spacer of the main Dolder bar effected the stress concentration labio-lingually.

While the torquing effect was greater in the model 2 (design with spacers only on the cantilevered extensions) and model 3 (resilient design) than in the model 1 (rigid design), the rigid design without spacer produced significantly greater labial torquing stresses than the resilient design with spacers on the surrounding structure of the implant fixture of the loaded side (fig. 10). The torquing stresses were produced on the disto-cervical contact point and labio-apical contact point. The fringe values on the disto-cervical contact point of the loaded side were unaffected by the bar joint design. However the greatest fringe values on the labio-apical contact point were obtained in the rigid design. The greatest torquing stress was caused by the rigid design on the disto-cervical contact point and labio-apical contact point between the implant and the surrounding structure.

In the pilot study a model with the Dolder bar without cantilever extensions generated more stress in the posterior ridge area. The results were similar to those reported by Thayer and Caputo.⁵ There was no stress concentration on the cervical region and the fringe values obtained in the apical region were significantly less than those from the model with cantilever extension in the main

study. The fringe values were almost half. Thayer and Caputo⁶ reported that the more retentive bar attachments for overdentures produced higher stress concentrations: our observation showed similar results. In our main study, more retentive multiple sleeve bar attachments with cantilever extensions produced higher stresses on the surrounding structure of the implant of the loaded side than the single sleeve Dolder bar attachment of the pilot study. The torquing stress in model 1 and 2 may exceed the physiological limit of osseointegration. It is apparent that cantilevered extensions possess considerable potential for the application of torque to the abutment and should be employed with care and discretion.

Three-dimensional photoelastic stress analysis affords a convenient method of visualizing and measuring stresses with a three-dimensional object such as the mandible used in this study. The experimental method used was relatively sensitive for evaluating stress applications resulting from three different designs of bar attachments. This method may be equally sensitive in evaluating other biomechanics of dental prostheses. The validity of the three-dimensional stress analysis was acceptable.

CONCLUSION

1. There were less stresses within the surrounding structure of the implants in the cervical regions than in the apical regions.
2. The fringes in the surrounding structure of the implants of the loaded sides were con-

siderably closer labio-lingually than mesio-distally.

3. Stresses induced by rigid design of the bar joint were higher than those induced by the resilient design.
4. Torquing stresses induced by cantilevered extensions were considerable and stresses were concentrated on the disto-cervical contact point and on the labio-apical contact point between the implant and the surrounding structure.

ACKNOWLEDGEMENT

We would like to thank Cendres & Metaux SA and Nobelphama AB for the supply of components.

REFERENCES

1. Bränemark RI, Hansson BO, Adell R, Breine U, Lindstrom J, Hallen O, Ohman A: Osseointegrated implants in the treatment of the edentulous jaw; Experiment from a 10-year period. *Scan J Plast Reconstr Surg Suppl* 1977;11:16.
2. Engquist B: Six years experience of splinted and non-splinted implants supporting overdentures in upper and lower jaws, Schepers E, Naert I, Theunciers CR (eds): *In overdentures and implants; an osseointegrated approach in overdentures on oral implants*. Leuven, Leuven University Press. 1991, PP 27-42.
3. Caputo AA, Standlee JP: *Biomechanics in clinical dentistry*. Chicago, Quintessence Co. 1989, PP 13-28.
4. Kinni ME, Hokama SN, Caputo AA: Force transfer by osseointegration implant devices. *Int J Oral Maxillofac Implant* 1987;2:11-14.
5. Thayer HH, Caputo AA: Photoelastic stress analysis of overdenture attachments. *J Prosthet Dent* 1980;43:611-617.
6. Thayer HH, Caputo AA: Occlusal force transmission by overdenture attachments. *J Prosthet Dent* 1979;41:266-271.

Reprint request :

Professor Sang Wan Shin, Department of Dentistry, Guro Hospital, Korea University Medical School, 80 GuroDong Seoul 152-050 Korea